J. Earth Syst. Sci. (2021)130 102
https://doi.org/10.1007/s12040-021-01596-0

Dimensionality and directionality analysis of magnetotelluric data by using different techniques: A case study from northern part of Saurashtra region, India

P V Vijaya Kumar[1,3,*], P B V Subba Rao[1], A K Singh[1], Amit Kumar[1] and P Rama Rao[2]

[1]*Indian Institute of Geomagnetism, Panvel, Navi Mumbai 410 218, India.*
[2]*Centre for Studies on Bay of Bengal, Andhra University, Visakhapatnam 530 003, India.*
[3]*Presently at NGRI, Hyderabad, India.*
**Corresponding author. e-mail: pvijaygeotech@gmail.com*

MS received 2 May 2019; revised 29 July 2020; accepted 6 February 2021

Magnetotelluric (MT) data has been collected along 32 stations along E–W profile in northern part and eight LMT (long period MT) stations in north-central part of Saurashtra region. Dimensionality analysis is carried out prior to MT modelling for obtaining the subsurface dimension as well as the direction of the underlying substructures. To estimate the subsurface dimensionality from MT data, different techniques Swift skew, Bhar's skew, normalized weights, phase tensor (PT) analysis and Wall's rotational invariant approach have been applied. These results suggest 1D structure for lower periods (0.01–1 s) and 3D structure for higher periods (1–10000 s) along two different profiles indicating that the study area is highly heterogeneous. Regional strike has been estimated through phase tensor (PT) and Groom–Bailey (GB) techniques suggests N40°E regional strike direction that correlates well with the Delhi–Aravalli tectonic trend. 2D modelling of MT/LMT data sets brings out different resistivity and conductivity blocks. Basaltic magmatic intrusion and its recrystallization have resulted in resistivity blocks with conductivity anomalies (trapped fluids) in between them. It has been reflected as 3D structures at higher periods. Different sedimentary basins at shallow depth are observed as 1D structure in dimensionality analysis.

Keywords. Magnetotellurics; dimensionality analysis; normalized weight index; phase tensor analysis; modelling.

1. Introduction

The magnetotelluric (MT) method (Vozoff 1991; Simpson and Bahr 2005) is a passive electromagnetic technique that is governed by diffusion Maxwell equations. MT experiment involves in measuring time-varying magnetic field components (B_x, B_y and B_z) and telluric field components (E_x and E_y) where x represents north–south, y is east–west, and z vertically downward components. Analysis of MT data is carried out in frequency domain and computations of cross-spectra/power spectra are carried out between (B_x and E_y) and (B_y and E_x) for different frequencies to determine impedance tensors (Z_{xx}, Z_{xy}, Z_{yx} and Z_{yy}). Apparent resistivity (ρ_{xx}, ρ_{xy}, ρ_{yx} and ρ_{yy}) and phases

Published online: 24 May 2021

($Ø_{xx}$, $Ø_{xy}$, $Ø_{yx}$ and $Ø_{yy}$) are estimated for different frequencies from these impedance tensors.

Observed MT responses are distorted due to cultural and geological noise. Local shallow small-scale conductivity anomalies can lead to galvanic distortions and/or current channelling causing frequency independent scaling of the MT resistivity curves leaving phases unchanged. These effects are normally minimized through tensor decomposition analyses and regional strike determination (Groom and Bailey 1989, 1991; McNeice and Jones 2001; Caldwell *et al.* 2004; Moorkamp 2007).

Dimensionality analysis is carried out prior to modelling for determining whether the computed impedance tensors, apparent resistivities and phases at a given frequency correspond to 1D, 2D or 3D geoelectrical structures. The main purpose of carrying out this analysis is to determine the variation of strike direction with depth or presence of surficial distorting bodies (Marquis *et al.* 1995; Marti *et al.* 2010). MT data interpretation is based on the dimensionality analysis, whether the structure is 1D, 2D or 3D. In this paper, dimensionality and directionality analysis have been applied for the MT/LMT data collected across the northern part of Saurashtra by using different techniques and compared with 2D models obtained after inversion.

2. Geology of Saurashtra Region

The Deccan trap basalts have erupted 65 Ma (Baksi 1987, 2014; Pande 2002; Chenet *et al.* 2008) on the Archean crust of the Indian shield (Chakrabarti and Basu 2006; Ray *et al.* 2008). These traps cover the older formations of Dharwar, Aravalli, Bastar and Bundelkhand cratons and the Satpura mobile belt (Bastia and Radhakrishna 2012) and occupy an area of ∼0.5 million km^2 in central and western parts of India. It is associated with the breakup of India from Seychelles (Norton and Sclater 1979; Courtillot *et al.* 1986; Royer *et al.* 1989). These traps have erupted in a span of 4–5 Ma during the Cretaceous–Tertiary boundary (Bhattacharji *et al.* 1996; Hofmann *et al.* 2000; Chenet *et al.* 2008).

Saurashtra region is covered by Deccan traps except along the coastal fringes where Tertiary and Quaternary sediments are exposed (as shown in figure 1).In the northern part of Saurashtra region, a small patch of Mesozoic sedimentary rocks are exposed. This region consists of several volcanic plugs (Porbander in SW, Junagadh in south and Palitana in SE) and is composed of acidic, alkaline and mafic/ultramafic rocks (Merh 1995; Sheth *et al.* 2012). To determine the complex geoelectrical structure beneath the trap-covered region of the northern part of Saurashtra, 32 MT stations and 8 LMT stations are deployed in an EW direction (along two profiles) covering different geological provinces as shown in figure 1.

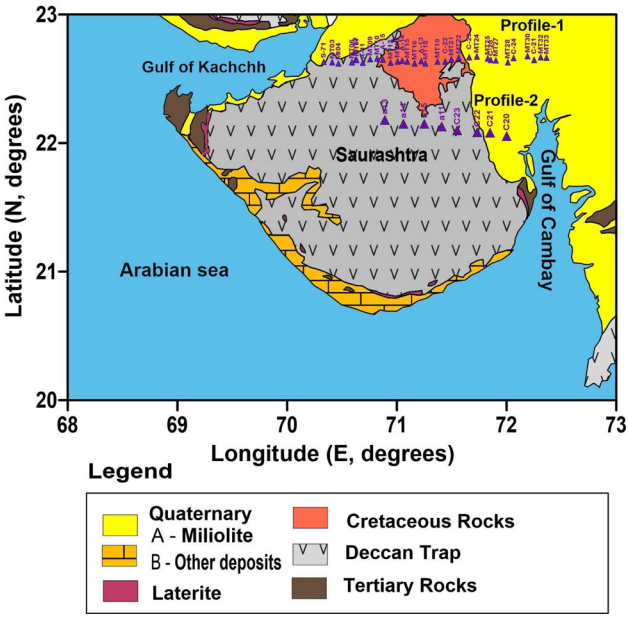

Figure 1. Geological map of Saurashtra and the surrounding regions (after GSI 1998) showing that entire region is covered by Deccan traps. Triangles indicated the two different MT/LMT profiles located in the northern part of Saurashtra region. Profile-2 contains LMT stations only.

3. MT data acquisition and processing

Regional MT/LMT data were acquired along a profile with MT station spacing around 6–8 km and LMT station at an interval of ∼15–20 km in the northern part of Saurashtra region as shown in figure 1. The MT data were collected in a frequency band 0.001–10000 Hz for a period of 36 hrs, whereas LMT data were collected in a period ranging from 10 to 30000 sec, for a period of 3–4 weeks. In the survey, two MTU-5A units were installed simultaneously about 6–8 km apart and are used as a remote reference station during data processing so as to remove noise and improve the quality of data (Gamble *et al.* 1979).

The MT time series data were processed by using SSMT 2000 software package available with Phoenix Geophysics system based on robust

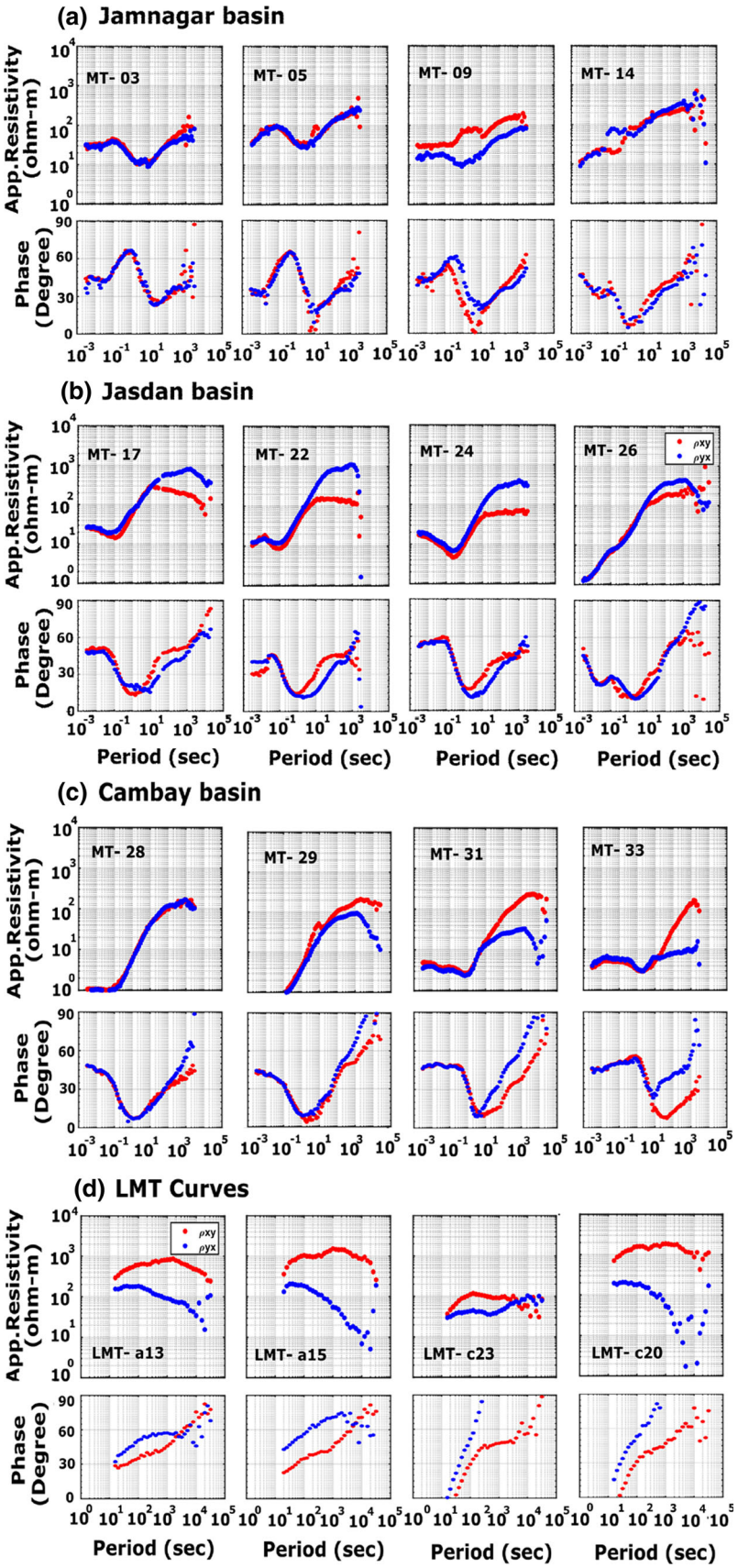

Figure 2. Apparent and phase curves obtained after remote reference technique, **(a)** MT03-MT14 over Jamnagar basin, **(b)** MT17-MT26 over Jasdan basin, **(c)** MT28-MT33 over western part of Cambay basin, and **(d)** LMT data acquired along profile-2 in the north-central part of Saurashtra region.

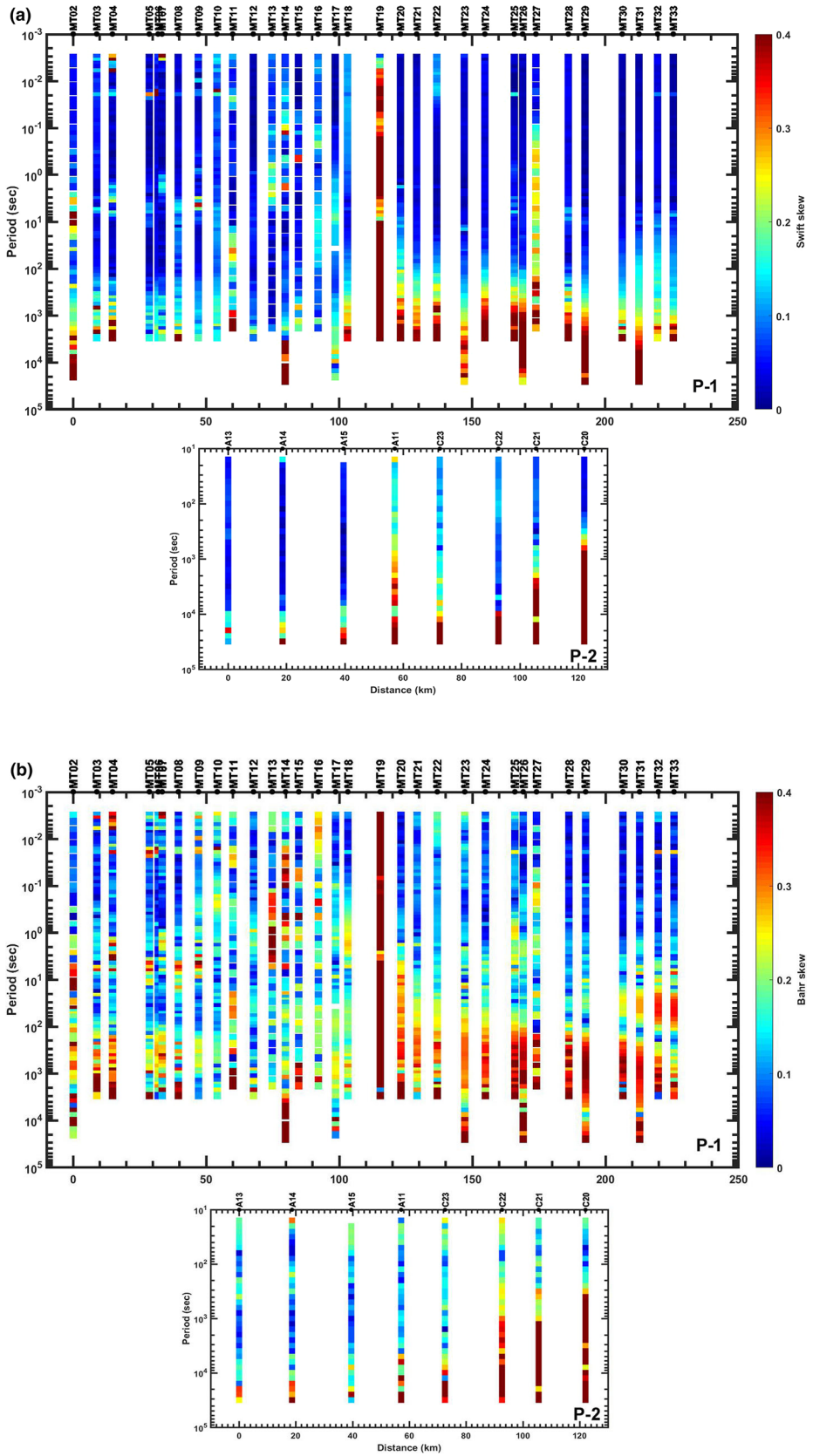

Figure 3. The variation of the **(a)** Swift skew and **(b)** Bahr skew with respective periods for different sites along the two different profiles (P-1 and P-2) indicating at higher periods, subsurface is showing 3D in nature.

reference cascade decimation technique (Jones and Jodicke 1984; Jones *et al.* 1989). LMT data were analyzed by using the LEMI LMT data processing software package supplied by LVIV Centre of Institute for Space Research. This software is built on the concepts of Egbert and Booker (1986) and Eisel and Egbert (2001). The processed MT/LMT apparent resistivity and phase curves along two profiles over different basins for selected stations are shown in figure 2(a–d).

MT data is presented in the form of apparent resistivity and phase's *vs.* frequency curves. This picture describes variation of apparent resistivity with frequency that is useful in qualitative interpretation. Figure 2(a) shows MT apparent and phase curves over Jamnagar basin. Stations MT-03, MT-05, MT-09 and MT-14 are located over Jamnagar basin. This basin is well reflected 10^{-2}–10^{0} Hz in all MT stations except at MT-14 that brings out a resistive block located close to Jasdan basin. Stations MT-17, 22, 24 and 26 are located over Jasdan basin (figure 2b). These curves show conducting sedimentary basin at high frequencies and resistivity increases with frequency. MT-28, 29, 31 and 33 are located over western part of Cambay basin (figure 2c). Low resistivities (1–5 Ωm) have been observed over Cambay sedimentary basin from frequency 10^{-3}–10^{-1} Hz and resistivity increases with frequency. Figure 2(d) shows LMT curves along profile-2. High resistivity is observed along all the LMT stations from 10^{-3} to 0.1 Hz and above 10^{-3} Hz shows a moderately conductive structure. Along the stations C23–C20, phases are distorted due to presence of highly conducting sediments at shallow depths within the Cambay basin. This causes anomalous phases that are produced due to higher resistivity contrast between basement and sedimentary basin (Lezaeta and Haak 2003; Selway *et al.* 2012).

4. Dimensionality analysis using different techniques

Prior to MT modelling, dimensionality analysis is carried out to determine whether the computed responses (from observed data at a selected frequency) correspond to 1D, 2D or 3D geoelectrical structures. It allows in identification and quantification of distortions (Groom and Bailey 1989; Smith 1995; McNeice and Jones 2001) and recovery of the strike of the subsurface structures (Marti *et al.* 2010). Different dimensionality methods are explained below.

4.1 *Swift and Bahr skew*

Skewness is the first parameter used in MT for determining the dimension of subsurface structures. The Swift skew (Swift 1967) uses MT impedance tensor and is based on the amplitude response tensor. The Swift skew is defined as follows:

$$\text{Swift skew} = \frac{(Z_{xx} + Z_{yy})}{(Z_{xy} - Z_{yx})}.$$

Drawback of the above method is that distortions are present due to coupling of the regional 1-D or 2-D inductive response with localized, small-scale conductive anomalies (Simpson and Bahr 2005). In order to overcome the drawbacks of Swift method in the presence of local distortions, Bahr (1991) has introduced skew values which depend on the phases of the impedance tensor that are not affected by amplitude distortion effects. The Bahr's phase-sensitive skew is given by

$$\text{Bahr's skew} = \frac{|[D_1 S_2] - [S_1 D_2]|^{1/2}}{|D_2|},$$

where

$S_1 = Z_{xx} + Z_{yy}$; $S_2 = Z_{xy} + Z_{yx}$,

$D_1 = Z_{xx} - Z_{yy}$; $D_2 = Z_{xy} - Z_{yx}$.

Generally, if skew values are >0.3, then it implies that the MT data are 3D. Swift and Bahr skew values were calculated for both the profiles in the northern part of Saurashtra region as shown in figure 3(a and b). At lower periods, skew values are < 0.3 indicating that the structure is 1D or 2D in nature. In both the profiles, at higher periods the skew values are > 0.3 indicating the 3D subsurface complex behaviour.

4.2 *Normalized dimensionality weights*

Noting the problems in Swift skew, Kao and Orr (1982) introduced a set of three normalized dimensional weights (D_1, D_2 and D_3). These weights deal with the amplitude of impedances (Z_1, Z_2, Z_3 and Z_4) that represent the relative weights of the dimensionality of 1-D, 2-D and 3-D structural contributions simultaneously. The relative weights D_1, D_2 and D_3 are given by

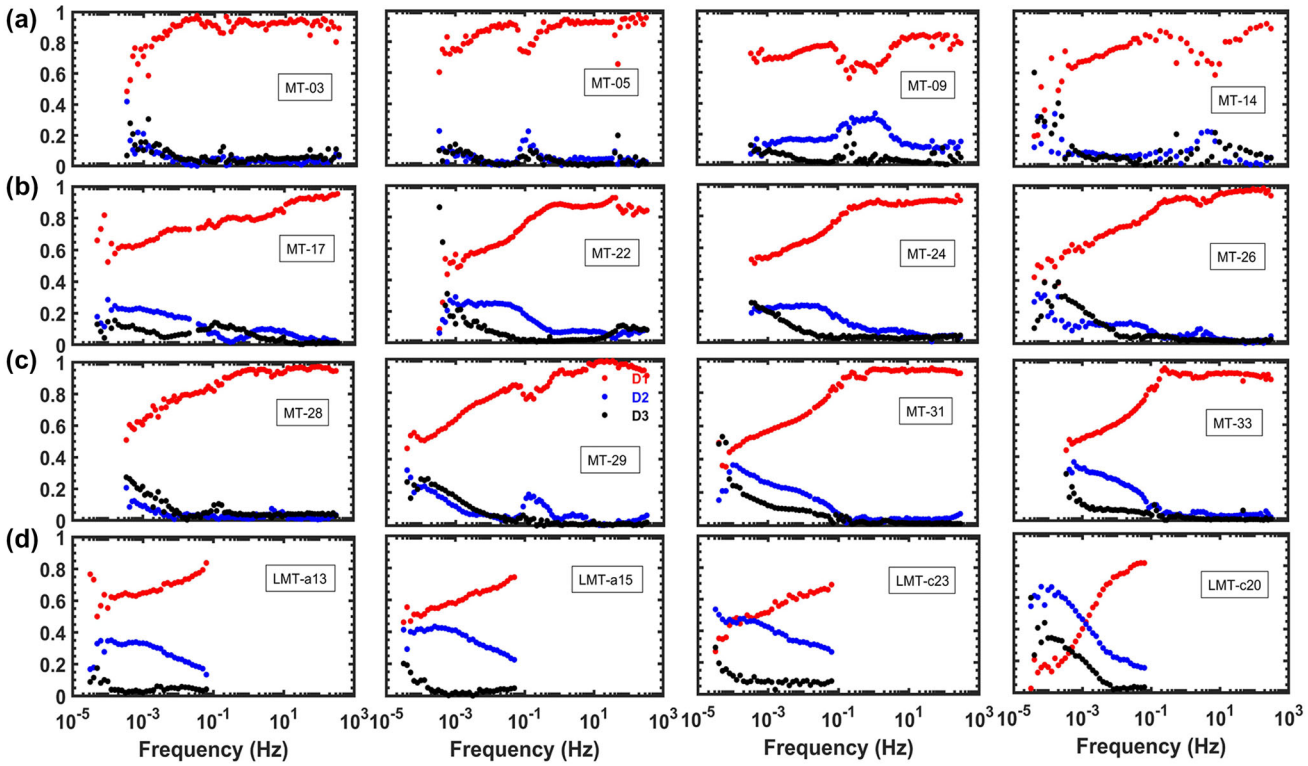

Figure 4. The normalized weights (D1, D2 and D3) with frequency for different sites over different basin as follows: **(a)** MT03-MT14 over Jamnagar basin, (**b**) MT17-MT26 over Jasdan basin, **(c)** MT28-MT33 over western part of Cambay basin, and (**d**) LMT stations along the profile-2 in the northern part of Saurashtra region.

$$D_1 = \frac{|z_1|}{\gamma}; \quad D_2 = \frac{|z_3|}{\gamma}; \quad D_3 = \frac{|z_2|}{\gamma},$$
$$\gamma = |z_1| + |z_3| + \frac{(|z_2 + z_4|)}{2}.$$

The above weights are expected to be in the range between 0 and 1, for 1D case, $D_1 > D_2 > D_3$. In case of 2D or 3D structure present, the values of D_2 and D_3 are greater than or nearly equal to the 0.2 where the $D_1 < D_2$. Northern part of Saurashtra MT/LMT profiles were investigated by using this technique, inferred the condition $D_1 > D_2 > D_3$ is true at all the sites for both the profiles over different basins (figure 4 a–d) and also at most of the sites the values of D_2 and D_3 are ≥ 0.2 indicates that at lower frequencies subsurface is 2D or 3D in nature. However, this analysis gives simultaneous qualitative assessment of the subsurface dimensionality that is useful in supporting the other methods.

4.3 *WALDIM analysis*

This method is known as Weaver, Agarwal and Lilley dimensionality analysis (Weaver *et al.* 2000). WALDIM analysis (Marti *et al.* 2009) is a numerical approach in which total seven independent (I_1, I_2, I_3, I_4, I_5, I_6, I_7) and one dependent (Q) invariants are analyzed based on the WAL invariant criteria (Weaver *et al.* 2000). Invariants I_3–I_7 and Q are used to determine the dimensionality and parameters necessary to correct galvanic distortion. The criteria for different dimensionality are shown in table 1 (after Marti *et al.* 2009). By using table 1 as a basic criterion, one can visualize from figure 5, that at high periodicity the subsurface is 3D or 3D/2D, and at lower periodicity, the subsurface is 1D in nature for the profile-1, whereas in profile-2 containing LMT data show a complex 3D subsurface structure.

4.4 *Phase tensor analysis*

Phase tensor (Caldwell *et al.* 2004; Moorkamp 2007) analysis is one of the important tools to analyse the dimensionality of the subsurface and is unaffected by any galvanic distortions. It gives distortion-free phase information on the regional scale. The phase tensor is defined by:

Table 1. *Different conditions for subsurface dimensionality based on WAL invariant values of the MT tensor (after Marti et al. 2009).*

I_3–I_7 and Q values	Geoelectric dimensionality
$I_3 = I_4 = I_5 = I_6 = 0$	1D
$I_3 \neq 0$ or $I_4 \neq 0$; $I_5 = I_6 = 0$; $I_6 = 0$ or Q=0	2D
$I_3 \neq 0$ or $I_4 \neq 0$; $I_5 \neq 0$; $I_6 = 0$; $I_7 = 0$	3D/2D twist 2D affected by galvanic distortion (only twist)
$I_3 \neq 0$ or $I_4 \neq 0$; $I_5 \neq 0$; $I_6 = 0$; Q=0	3D/1D2D Galvanic distortion over 1D or 2D (Non-recoverable strike direction)
$I_3 \neq 0$ or $I_4 \neq 0$; $I_5 = I_6 = 0$; $I_7 = 0$ or Q=0	3D/1D2D Galvanic distortion over 1D or 2D Resulting in a MT diagonal tensor
$I_3 \neq 0$ or $I_4 \neq 0$; $I_5 \neq 0$; $I_6 \neq 0$; $I_7 = 0$	3D/2D General case of galvanic distortion over a 2D structure
$I_7 \neq 0$	3D (affected or not by galvanic distortion)

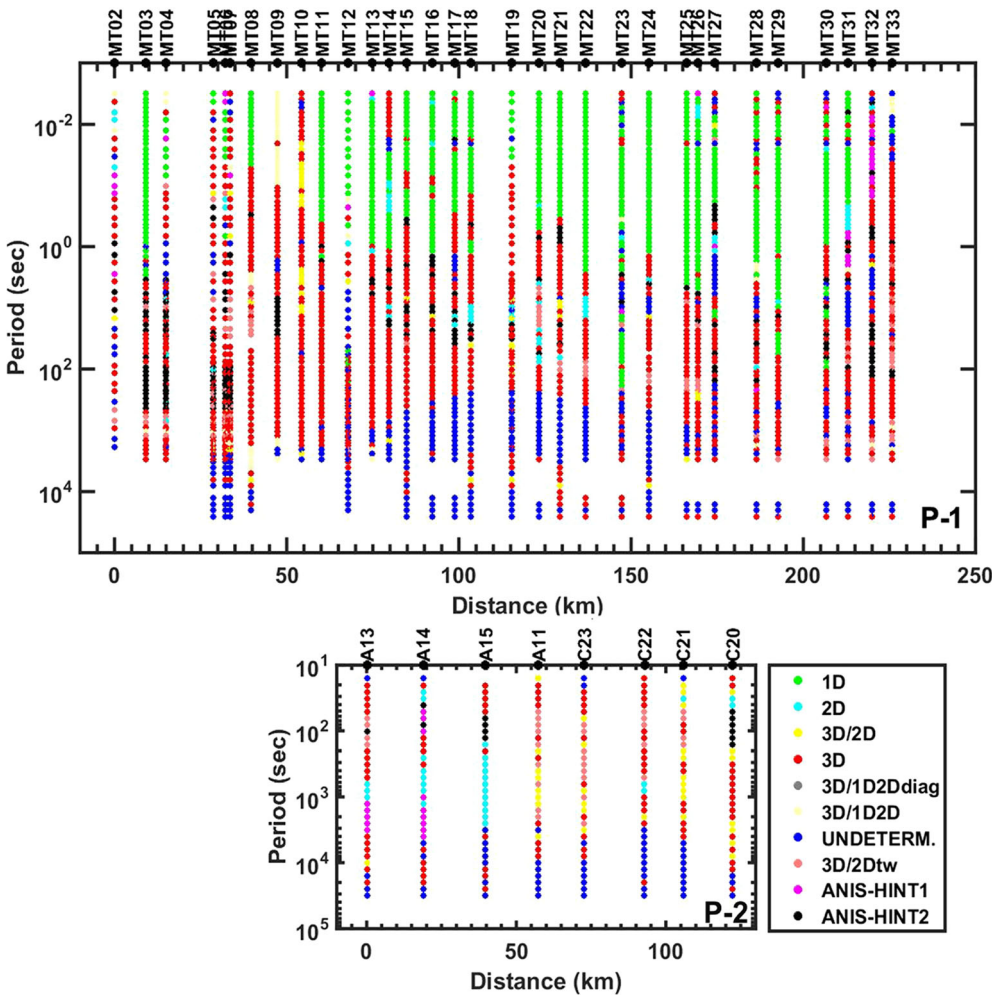

Figure 5. WALDIM dimensionality analysis implemented for two different profiles (P-1 and P-2) in the northern part of Saurashtra at each site for complete periodicities. At higher periodicity, MT data significantly shows that subsurface is 3D in nature.

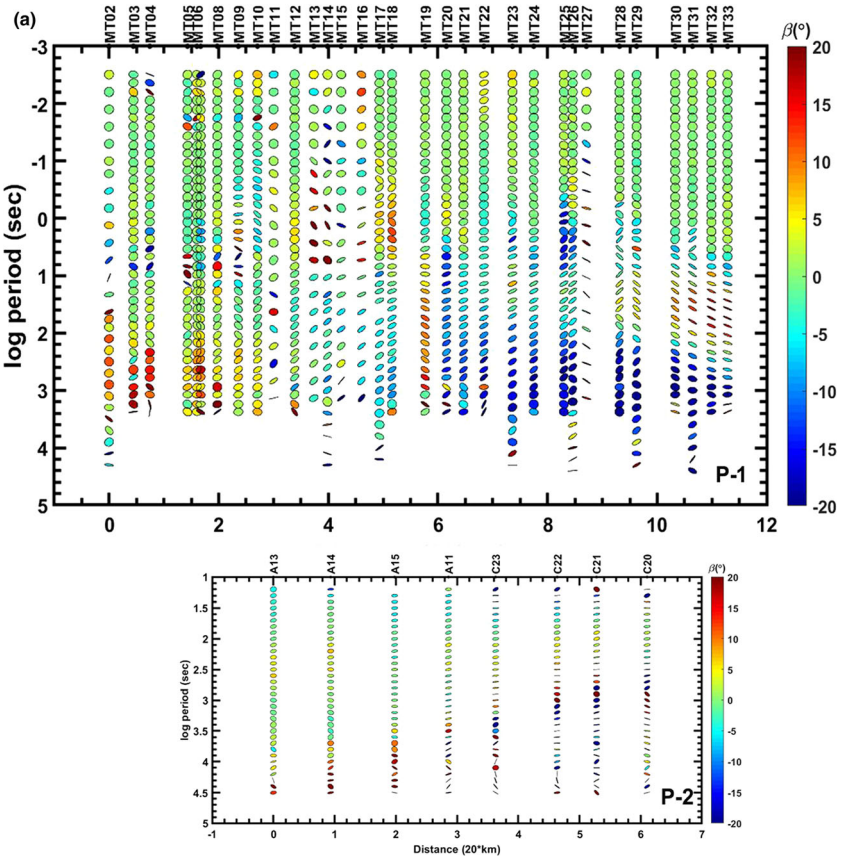

Figure 6. **(a)** Shows the subsurface heterogeneity using β values. At higher periods, β value exceeds $\pm 5°$ indicates 3D subsurface. **(b)** The ellipses are plotted so that the vertical axis corresponds to an NE–SW orientation. The minimum phase is < 50 corresponds to a resistive block that corresponds to a recrystallized magma related to hotspot activity. **(c)** Phase tensor ellipses along the profile for all periods, for short periods (0.1–100 s) the phase angle between electric and magnetic fields ($\Phi_{\max}$) is low, indicating a high resistive block correlating with (b). **(d)** Also shows high resistive mid-crustal layer as observed in (b and c).

$$\Phi = X^{-1}\,Y = \begin{bmatrix} Z_{xx} & Z_{xy} \\ Z_{yx} & Z_{yy} \end{bmatrix}.$$

where X and Y are the real and imaginary parts of the impedance tensor (Z). It is represented as an ellipse with maximum phase as an ellipse major axis ($\Phi_{\max}$) and ellipse minor axis ($\Phi_{\min}$) for the minimum phase. Caldwell *et al.* (2004) defined a parameter skew (β) which defines the inherent dimensionality of the subsurface. It is represented as follows:

$$\beta = 0.5\,\tan^{-1}\left(\frac{\Phi_{12} - \Phi_{21}}{\Phi_{11} + \Phi_{22}}\right).$$

In case of 1D, the phase tensor ellipse more or less is equal to circle, because $\Phi_{\max}$ and $\Phi_{\min}$ are almost equal and skew (β) is also zero. For 2D structures, $\Phi_{\max}$ and $\Phi_{\min}$ are different with skew (β) equal to zero is a necessary condition, but not sufficient (Caldwell *et al.* 2004). If the major axis of the phase tensor ellipse is rotated by the angle α (geoelectrical strike angle), then the major axis of the phase tensor ellipse is aligned parallel or perpendicular to the regional strike direction denoting 90° ambiguities corresponding to the TE or TM mode. The skew angle β measures the deviation from two-dimensionality and it represents 'quasi-2D' (if $|\beta| < 3°$). In case of 3D, β is non-zero and the direction of the major axis is given by the angle α–β.

Figure 6 shows the colour filled phase tensor ellipses along the two profiles. The four colour schemes used to characterize the subsurface dimensionality or heterogeneity β (figure 6a); arctan ($\Phi_{\min}$) (figure 6b); $\Phi_{\max}$ (figure 6c) and $\Phi_{\min}$ (figure 6d). At short periods, the phase tensors are nearly circle along the profile, indicating 1D structure. As periodicity increases, these circles become ellipse and asymmetry in the regional MT response due to mid-crustal inhomogeneities. In the mid-crustal level, low phase angles (arctan($\Phi_{\min}$), $\Phi_{\max}$, and $\Phi_{\min}$) are corresponding to 2D structure. At lower frequencies $|\beta|$ is greater

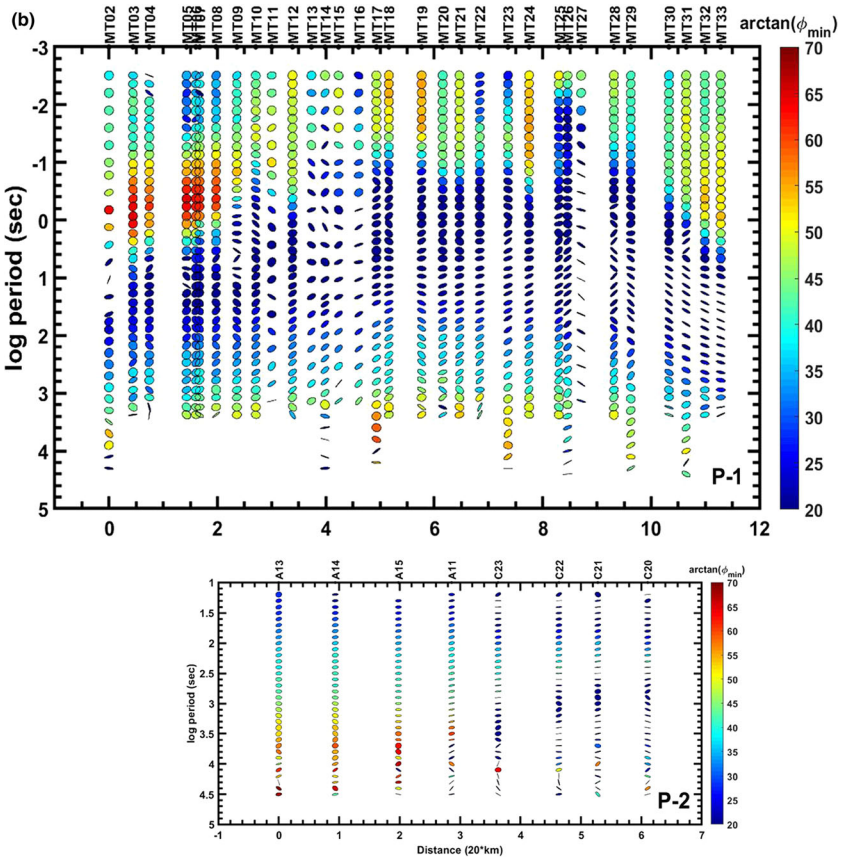

Figure 6. (*Continued.*)

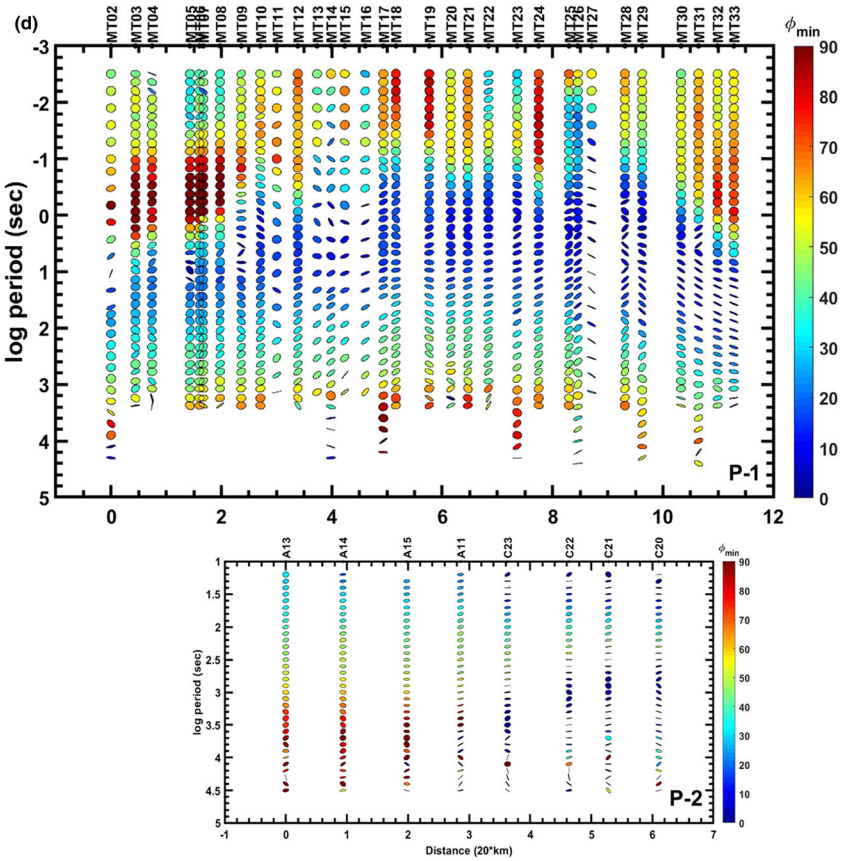

Figure 6. (*Continued.*)

than or less than 5° indicating that the subsurface structure is 3D. The low phase angle (Φ_{max} and Φ_{min}) is corresponding to the rapid change in resistivity (Stagpoole *et al.* 2009). This low phase angle correlates well with a recrystallized older Precambrian crust that forms the uplifted blocks derived from the lithospheric mantle along profile-1 (Vijaya Kumar *et al.* 2018, 2020). Similar results are obtained along LMT profile-2.

4.5 *Strike analysis*

Obtaining the strike direction is one of the important criteria before modelling the MT response. In order to obtain strike direction, we have utilized two different methods such as Groom–Bailey (GB) and phase tensor (PT) as shown in figure 7. In figure 7(a and b), the strike direction obtained for the profile-1 by using GB and PT analysis is shown. Regional strike N40°E coincides with Delhi–Aravalli trend. Strike obtained for the profile-2 by using GB and PT analysis is shown in figure 7(c and d). Here, the strike direction obtained from GB is different from PT analysis as station spacing along profile-2 is more than 20 km. Thus, we have adopted N40°E as a regional strike for 2D analysis.

5. 2D inversion

For 2D modelling/inversion, the MT impedance tensor is decomposed into two independent (TE and TM) modes. In the transverse electric (TE) mode, electric field is measured parallel to geoelectrical strike, while the magnetic field is perpendicular. Whereas in the transverse magnetic (TM) mode, magnetic field is parallel to the geoelectrical strike and electric field is measured perpendicular to strike. The decomposed responses of TE and TM mode data were inverted by using the non-linear conjugate gradients (NLCG) algorithm of Rodi and Mackie (2001) as implemented in the WinGLink software package. Thus, the subsurface resistivity model is obtained by jointly inverting TE and TM mode apparent resistivity and phase data using the above inversion.

As TE mode data is sensitive to localized heterogeneities than TM mode data, more

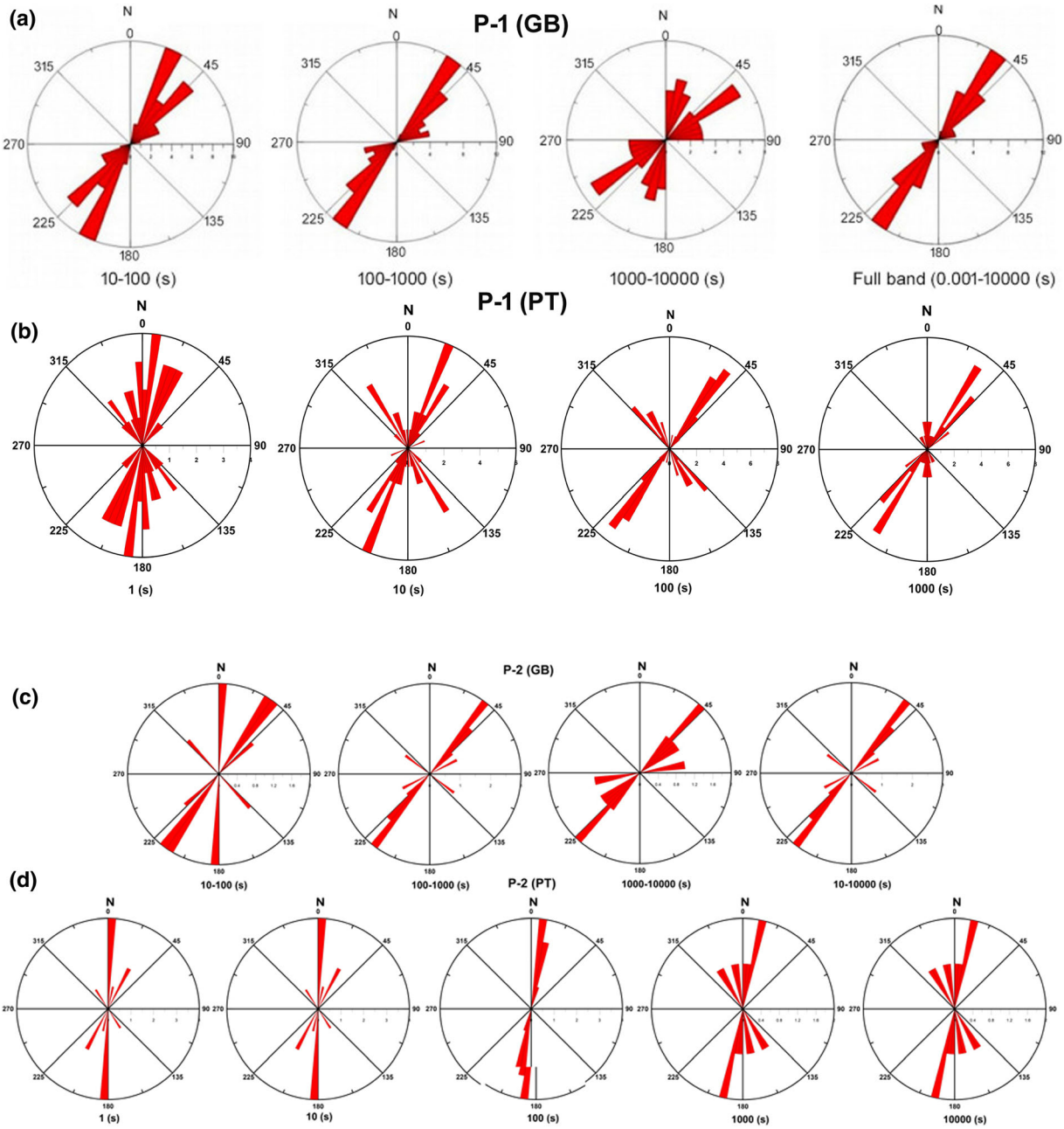

Figure 7. **(a** and **b)** Rose diagram plot of regional strike direction for broad period through Groom-Bailey decomposition (GB) and phase tensor (PT) techniques for the profile-1. In these analyses, regional strike obtained by above techniques is about N40° E. (**c** and **d**) are the strike direction for LMT data through (GB) and phase tensor (PT) techniques for the profile-2. In this case, regional strike obtained by GB analysis is about N40° E and by PT it is about N20° E. This ambiguity may be due to large station spacing between LMT sites.

importance is given to TM mode to avoid these inherent effects which cause poor data fit in TE mode (e.g., Jones 1983; Wannamaker *et al.* 1997; Ledo *et al.* 2002; Ledo 2005). The dimensionality analysis suggests that the presence of 3D structures at higher periods along the profile-2. In the case of TM mode, the current flows across the boundaries of different structures permit to build charges on the interfaces helps in locating complex structures (Berdichevsky 1999; Ledo *et al.* 2002, 2005; Liang *et al.* 2015). Thus, in the presence of 3D conductivity structures, TM mode is an efficient mode to locate the subsurface resistivity structures. Hence, we have interpreted TM mode data along profile-2. Details of modelling for the profile-1 are discussed by Vijay Kumar *et al.* (2018). Interpreted model is shown in figure 9(a). In the present work, 2D inversion of LMT data collected along profile-2 has

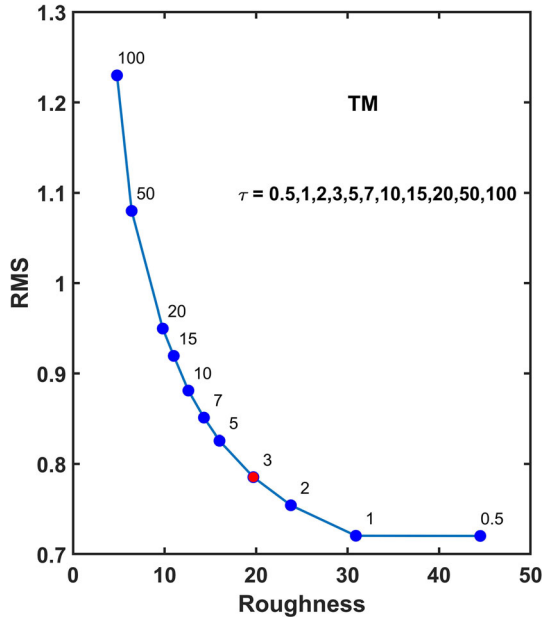

Figure 8. L curve represents the roughness *vs.* RMS misfit for different regularization parameters used for 2D inversion of the Profile-2. τ=3 is adopted for final model.

been worked out. Error floor for resistivity is given as 10% and for phases it is about 5% (for TM mode data). Initially, we have used 100 Ωm uniform resistivity half-space as an initial model mesh containing 59 rows and 123 columns for obtaining geoelectrical model. Different models were generated by using different smoothing parameters (τ) varying from 1 to 100. When plotted as an L-curve, it has been found that τ=3 can be considered as a preferred value of the trade-off parameter (figure 8) for inversion. Inversion model obtained after 100 iterations with an RMS misfit of 0.758 is shown in figure 9(b) (for TM data). Comparison between observed and calculated apparent and phase curves are shown in figure 10. Dots signify observed curves, whereas solid line shows calculated denoting that overall data matching is in good agreement. Interpreted model brings out different resistivity and conductivity structures that correlate well with the model as shown in figure 9(a). These results are discussed below.

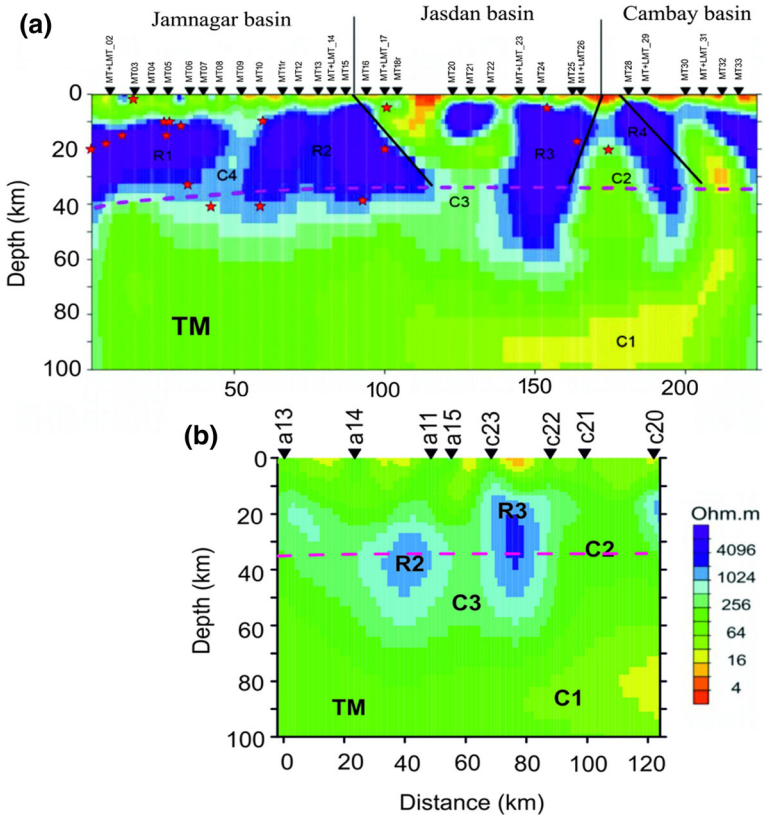

Figure 9. **(a)** Two-dimensional geoelectrical model derived from TM data along the profile-1 delineated different hidden basins (Jamnagar, Jasdan and Cambay) beneath the northern part of Saurashtra region underline by different resistive and conductive blocks. **(b)** Interpreted model across profile-2 brings out different resistive blocks R2 and R3 with a conductive zone C3 beneath Jasdan basin. C2 and C3 are mid-crustal conductivity anomalies that have been attributed to carbonate fluids. C1 is a moderate conductive anomaly in a depth range of about 80–100 km related to partial melting of lithosphere. The dashed line in two profiles denotes the Moho configuration obtained from seismological studies (Chopra *et al.* 2014).

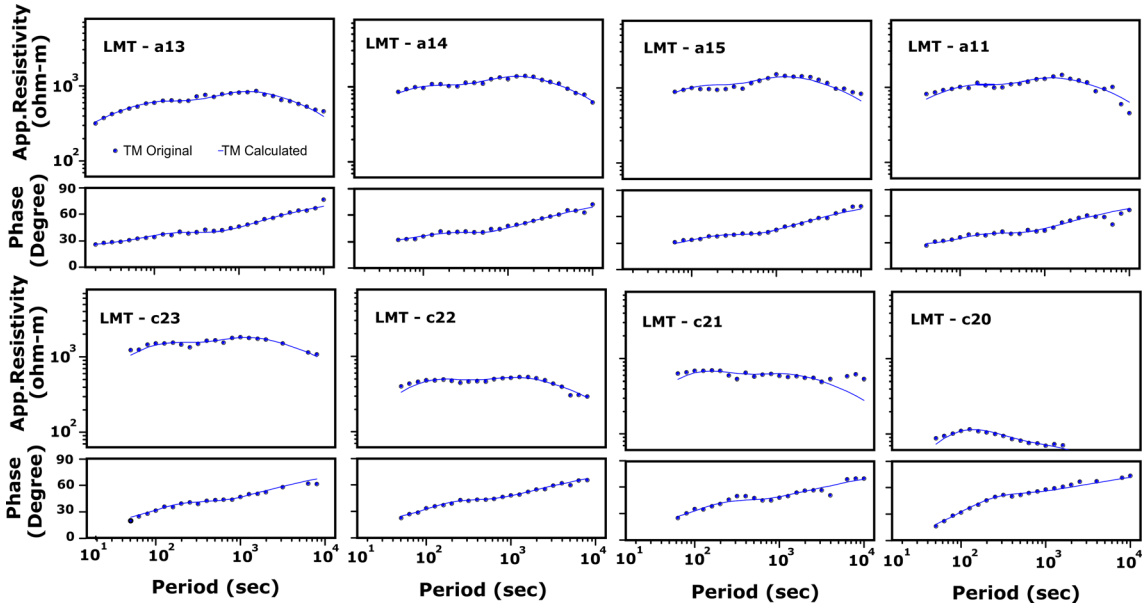

Figure 10. Comparison between observed and calculated responses (TM mode) for apparent resistivity and phase along the profile-2.

6. Results and discussion

Dimensionality of regional subsurface structure is obtained by Swift's skew and Bahr's skew. Swift skew values are found to be ≤2 for a period range of 10^{-3} to 10^{2} s suggesting 1D/2D nature of the structure. Above this period range, it suggests 3D nature of the structure. Similar results are also observed in Bahr's skew. Using normalized weights, it is suggested that the structure is 1D in nature for a period range of 10^{-3}–10^{2} s and beyond this range, it is 2D/3D in nature. WALDIM code (Weaver *et al.* 2000) has been utilized for performing the dimensionality analysis of the northern part of Saurashtra region. Weaver *et al.* (2000) presented a dimensionality study based on sets of rotationally invariant scalars computed from the observed MT impedance tensor. It brings out 1D substructure for a period range of 10^{-3} to 1 s and 3D nature for periods above 1s.

Phase tensor ellipse calculated for a period range of 10^{-3} to 1600 s is shown in figure 6(a–d). 1D, 2D and 3D structures are classified based on lambda and beta values (Bibby 2005). Based on the notation given by Bibby (2005), the calculated phase tensor ellipse for a period range 10^{-3} to 1 s is close to the circular which indicates 1D subsurface structure, later these circular patterns become ellipses with major axis aligning in NE–SW direction and suggests 3D nature. This NE–SW trend is consistent with Delhi–Aravalli trend. Overall dimensionality analysis suggests that shallow structure is 1D in nature and at higher periods, it is 3D in nature.

Strike angle plays an important role in modelling the MT data (Jones and Groom 1993). In the present study, strike direction is estimated through phase tensor (PT) and Groom–Bailey (GB) techniques. Regional strike assessed through PT and GB techniques suggests an N40°E direction and is consistent with the Delhi–Aravalli tectonic trend. MT data has been rotated by N40°E and 2D modelling brings out different resistive and conductive blocks that are discussed below.

It is well known that Deccan volcanic province (DVP) forms one of the Large Igneous Provinces (LIPs) with tholeiitic magmas (Chenet *et al.* 2008) that have erupted through different fissures (Nair and Bhusari 2001). These magmatic intrusions are related to decompression melting of an abnormally hot mantle material brought to the base of the lithosphere (Armitage *et al.* 2010). Thus, conductivity anomaly C1 and moderate resistivity values in a depth range of about 80–100 km in both profiles may be attributed to partial melting that causes subcrustal melting and significant alteration of the lithosphere. This anomaly C1 is also located close to the track of Reunion hotspot along the eastern edge of the Saurashtra (Campbell and Griffiths 1990) and correlates well with the low seismic velocity zone (LVZ) inferred from seismic tomography studies (Kennett and Widiyantoro 1999; Madhusudhan Rao *et al.* 2013, 2015; Kumar *et al.* 2016). Thus, the rising plume activity at

upper mantle depths may have formed enriched melts at the base of the lithosphere producing conductivity anomaly C1.

The above magmatic intrusions have propagated to the lower crust from deep within the lithosphere based on geochemical analysis (Karmalkar *et al.* 2008; Vijaya Kumar *et al.* 2010, 2017). High conductivity anomalies C2 and C3 in both profiles are attributed to carbonate fluids. These volatile fluids (H_2O and CO_2) are released upon crystallization of basaltic underplated material (Frost *et al.* 1989; Wannamaker *et al.* 1997; Bolongo *et al.* 2013; Vijaya Kumar *et al.* 2018; Nagarjuna *et al.* 2020). Linear conductive anomaly C4 in profile-1 may represent the electrical image of major fault/fracture zones of crustal scale through which Deccan volcanism may have taken place and could be related to dehydration of minerals during metamorphism (Byerlee 1993). According to Vijaya Kumar *et al.* (2018), conductivity anomaly A in profile-1 is associated with interconnected melts that have been fed to crustal layers by asthenospheric upwelling and underplated at the lower crust as magma chambers.

In both profiles, resistivity blocks R2 and R3 form the western and eastern fringe of Jasdan basin with a conductivity block C3 in between them. These blocks may represent older (Precambrian) crust existing before the Deccan volcanism as inferred from seismic tomography studies based on high Poisson's ratio (Praveen Kumar and Mohan 2014; Chopra *et al.* 2014). Later, mafic/ultramafic intrusions due to Reunion hotspot activity (Biswas 2005; Chatterjee and Bhattacharji 2008; Sheth *et al.* 2013; Mukherjee *et al.* 2017) and recrystallization of these blocks may have given rise to high resistive values indicating heterogeneity within the crust (Vijaya Kumar *et al.* 2018). Similarly, in profile-1, resistivity blocks R1 and R2 form the fringes of Jamnagar basin, whereas R4 in profile-1 is observed beneath the western part of Cambay basin. These conductive and resistive blocks have been reflected as 3D structures in dimensionality analysis.

7. Conclusion

This paper has used different techniques to differentiate the geoelectrical dimensionality of two profiles in northern part of Saurashtra. This analysis denotes that the crust beneath Saurashtra region is highly heterogeneous with near surface 1D effects, whereas at middle and lower depths 3D effects are observed.

Sedimentary basins at shallow depth have been reflected as 1D structure. Resistivity blocks (R1–R4) with conductivity blocks (C2–C4) in between them from mid-lower crust are reflected as 3D structures. Moreover, induced currents are deflected by resistive volcanic plugs causing current concentration in conductivity bodies leading to out of quadrant phase (Weidelt 1977; Jones 1983). As current channelling is difficult to explain by 1D and 2D models, it is considered to be 3D nature and requires complex 3D modelling.

Acknowledgements

The authors are very much grateful to Prof D S Ramesh, Director, IIG, for his constant encouragement and permission to publish this paper. We would like to thank Dr Prasanta K Patro, CSIR-NGRI for fruitful discussions. We thank anonymous reviewers and editor for their constructive comments that have enhanced the quality of the manuscript. Special thanks to Mr N K Gadai and other colleagues of Rajkot Magnetic Observatory, Saurashtra University, for logistic support during the entire field journey. Field support received from Mr D Nagarjuna is gratefully acknowledged.

Author statement

Both PVVK and PBVSR selected the datasets, performed the statistical analysis and carried out 2D inversion and drafted the manuscript. PRR has supervised the work. AKS and AK have taken part in MT field work.

References

Armitage J J, Collier J S and Minshull T A 2010 The importance of rift history for volcanic margin formation; *Nature* **465** 913–917.

Baksi A K 1987 Critical evaluation of the age of the Deccan Traps, India: Implications for flood-basalt volcanism and faunal extinctions; *Geology* **15** 147–150.

Baksi A K 2014 The Deccan Trap–Cretaceous–Paleogene boundary connection; new $^{40}Ar/^{39}Ar$ ages and critical assessment of existing argon data pertinent to this hypothesis; *J. Asian Earth Sci.* **84** 9–23.

Bastia R and Radhakrishna M 2012 Basin evolution and petroleum prospectivity of the Continental Margins of India; *Dev. Petrol. Sci.* **59** 1–417.

Berdichevsky M N 1999 Marginal notes on magnetotellurics; *Surv. Geophys.* **20** 341–375.

Bhatacharji S, Chatterjee N, Wampler J M, Nayak P N and Deshmukh S S 1996 Indian intraplate and continental margin rifting, lithospheric extension, and mantle upwelling in Deccan Flood Basalt Volcanism near the K/T Boundary: Evidence from mafic dike swarms; *J. Geol.* **104** 379–398.

Bibby H M, Caldwell T G and Brown C 2005 Determinable and non-determinable parameters of galvanic distortion in magnetotellurics; *Geophys. J. Int.* **163** 915–930.

Biswas S K 2005 A review of structure and tectonics of Kutch basin, western India, with special reference to earthquakes; *Curr. Sci.* **88** 1592–1600.

Bolongo M S, Nunes H O, Padilha A L, Vitorello I and Padua M B 2013 Anomalous electrical structure in the northwestern Paraná Basin, Brazil, observed with broadband magnetotellurics; *J. S. Am. Earth Sci.* **42** 74–82.

Byerlee J D 1993 Model for episodic flow of high-pressure water in fault zones before earthquakes; *Geology* **21** 303–306.

Caldwell T G, Bibby H M and Brown C 2004 The magnetotelluric phase tensor; *Geophys. J. Int.* **158** 457–469.

Campbell I H and Griffiths R W 1990 Implications of mantle plume structure for the evolution of flood basalts; *Earth Planet. Sci. Lett.* **99** 79–93.

Chatterjee N and Bhattacharji S 2008 Trace element variations in Deccan basalts: Roles of mantle melting, fractional crystallization and crustal assimilation; *J. Geol. Soc. India* **71** 171–188.

Chakrabarti R and Basu A R 2006 Trace element and isotopic evidence for Archean basement in the Lonar crater impact breccias, Deccan Volcanic Province; *Earth Planet. Sci. Lett.* **247** 197–211.

Chenet A L, Fluteau F, Courtillot V, Gerard M and Subbarao K V 2008 Determination of rapid Deccan eruptions across the Cretaceous–Tertiary boundary using paleomagnetic secular variation: Results from a 1200-m thick section in the Mahabaleshwar escarpment; *J. Geophys. Res.* **113** B04.

Chopra S, Chang T M, Saikia S, Yadav R B S, Choudhury P and Roy K S 2014 Crustal structure of the Gujarat region, India: New constraints from the analysis of teleseismic receiver functions; *J. Asian Earth Sci.* **96** 237–254.

Courtillot V, Besse J, Vandamme D, Montigny R, Jaeger J and Cappetta H 1986 Deccan flood basalts at the Cretaceous/Tertiary boundary?; *Earth Planet. Sci. Lett.* **80** 361–374.

Egbert G D and Booker J R 1986 Robust estimation of geomagnetic transferfunctions; *Geophys. J. Roy. Astron. Soc.* **87** 173–194.

Eisel M and Egbert G D 2001 On the stability of magnetotelluric transfer function estimates and the reliability of their variances; *Geophys. J. Int.* **144** 65–82.

Frost B R, Fyfe W S, Tazaki K and Chan T 1989 Grain-boundary graphite in rocks and implications for high electrical conductivity in the lower crust; *Nature* **340** 134–136.

Gamble T D, Goubau W M and Clarke J 1979 Error analysis for remote reference magnetotellurics; *Geophysics* **44** 959–968.

Groom R W and Bailey R C 1991 Analytic investigations of the effects of near-surface three-dimensional galvanic scatterers on MT tensor decompositions; *Geophysics* **56** 496–518.

Groom R W and Bailey R C 1989 Decomposition of magnetotelluric impedance tensors in the presence of local three-dimensional galvanic distortion; *J. Geophys. Res.* **94** 1913–1925.

Hofmann C, Feraud G and Courtillot V 2000 $^{40}Ar/^{39}Ar$ dating of mineral separates and whole rocks from the Western Ghats lava pile: Further constraints on duration and age of the Deccan traps; *Earth Planet. Sci. Lett.* **180** 13–27.

Jones A G 1983 The problem of current channelling: A critical review; *Surv. Geophys.* **6** 79–122.

Jones A G, Chave A D, Egbert G, Auld D and Bahr K 1989 A comparison of techniques for magnetotelluric response function estimation; *J. Geophys. Res.* **94** 14,201–14,213.

Jones A G and Jodicke H 1984 Magnetotelluric transfer function estimation improvement by a coherence-based rejection technique; In: SEG Technical Program Expanded Abstracts 1984, Society of Exploration Geophysicists, pp. 51–55.

Kao D and Orr D 1982 Magnetotelluric studies in the Market Weighton area of eastern England; *Geophys. J. Roy. Astron. Soc.* **70** 323–337.

Karmalkar N R, Kale M G, Duraiswami R A and Jonalgadda M 2008 Magma underplating and storage in the crust-building process beneath the Kutch region, NW India; *Curr. Sci.* **94** 1582–1588.

Kennett B L N and Widiyantoro S 1999 A low seismic wave speed anomaly beneath northwestern India: A seismic signature of the Deccan plume?; *Earth Planet. Sci. Lett.* **165** 145–155.

Kumar P, Sen G and Mandal P *et al.* 2016 Shallow lithosphere-asthenosphere boundary beneath Cambay Rift Zone of India: Inferred presence of carbonated partial melt; *J. Geol. Soc. India* **88** 401–406, https://doi.org/10.1007/s12594-016-0503-9.

Lezaeta P and Haak V 2003 Beyond magnetotelluric decomposition: Induction, current channelling, and magnetotelluric phases over 90; *J. Geophys. Res.* **108** 2305, https://doi.org/10.1029/2001JB000990.

Ledo J, Queralt P, Martí A and Jones A G 2002 Two-dimensional interpretation of three-dimensional magnetotelluric data: An example of limitations and resolution; *Geophys. J. Int.* **150** 127–139.

Ledo J 2005 2-D versus 3-D magnetotelluric data interpretation; *Surv. Geophys.* **26** 511–543.

Liang H D, Gao R, Hou H S, Liu G X, Han J T and Han S 2015 Lithospheric electrical structure of the Great Xing'an Range; *J. Asian Earth Sci.* **113** 501–507.

Madhusudhan Rao K, Ravi Kumar M, Singh A and Rastogi B K 2013 Two distinct shear wave splitting directions in the northwestern Deccan volcanic province; *J. Geophys. Res. Solid Earth* **118** 5487–5499.

Madhusudhan Rao K, Kumar M R and Rastogi B K 2015 Crust beneath the northwestern Deccan Volcanic Province, India: Evidence for uplift and magmatic underplating; *J. Geophys. Res. Solid Earth* **120** 3385–3405.

Marquis G, Jones A G and Hyndman R D 1995 Coincident conductive and reflective middle and lower crust in southern British Columbia; *Geophys. J. Int.* **120** 111–131.

Marti A, Queralt P and Ledo J 2009 WALDIM: A code for the dimensionality analysis of magnetotelluric data using the rotational invariants of the magnetotelluric tensor; *Comput. Geosci.* **35** 2295–2303.

Martí A, Queralt P, Ledo J and Fariaquharson C 2010 Dimensionality imprint of electrical anisotropy in magnetotelluric responses; *Phys. Earth Planet. Int.* **182** 139–151.

McNeice G W and Jones A G 2001 Multisite, multifrequency tensor decomposition of magnetotelluric data; *Geophysics* **66** 158–173.

Mehr S S 1995 Geology of Gujarat. Geological Society of India Publication, Bangalore, pp. 1–170.

Moorkamp M 2007 Comment on '*The magnetotelluric phase tensor*' by T. Grant Caldwell, Hugh M. Bibby and Colin Brown; *Geophys J. Int.* **171** 565–566.

Mukherjee S, Misra A A, Calvès G and Nemčok M 2017 Tectonics of the Deccan large igneous province: An introduction; *Geol. Soc. London Spec. Publ.* **445** 1–9.

Nagarjuna D, Rao C K, Amit Kumar, Rama Rao P and Subba Rao P B V 2020 Implications for the lithospheric structure of Cambay rift zone, western India: Inferences from a magnetotelluric study; *Geosci. Front.* **4** 5, https://doi.org/10.1016/j.gsf.2020.01.014.

Nair K K K and Bhusari B 2001 Stratigraphy of Deccan Traps: A review; *Geol. Surv. India, Spec. Publ.* **64** 477–492.

Norton I O and Sclater J G 1979 A model for the evolution of the Indian Ocean and the breakup of Gondwanaland; *J. Geophys. Res.* **84** 6803–6830.

Pande K 2002 Age and duration of the Deccan Traps, India: A review of radiometric and paleomagnetic constraints; *J. Earth Syst. Sci.* **111** 115–123.

Praveen Kumar K and Mohan G 2014 Crustal velocity structure beneath Saurashtra, NW India, through waveform modelling: Implications for magmatic underplating; *J. Asian Earth Sci.* **79** 173–181.

Ray R, Shukla A D, Sheth H C, Ray J S, Duraiswami R A, Vanderkluysen L, Rautela C S and Mallik J 2008 Highly heterogeneous Precambrian basement under the central Deccan Traps, India: Direct evidence from xenoliths in dykes; *Gondwana Res.* **13** 375–385.

Royer J Y, Sclater J G and Sandwell D T 1989 A preliminary tectonic fabric chart of the Indian Ocean; *Proc. Indian Acad. Sci.-Earth Planet. Sci.* **98** 7–24.

Selway K, Thiel S and Key K 2012 A simple 2-D explanation for negative phases in TE magnetotelluric data; *Geophys. J. Int.* **188** 945–958.

Sheth H C, Choudhary A K, Cucciniello C, Bhattacharyya S, Laishram R and Gurav T 2012 Geology, petrochemistry, and genesis of the bimodal lavas of Osham Hill, Saurashtra, northwestern Deccan Traps; *J. Asian Earth Sci.* **43** 173–192.

Sheth H C, Zellmer G F, Kshirsagar P V and Cucciniello C 2013 Geochemistry of the Palitana flood basalt sequence and the Eastern Saurashtra dykes, Deccan traps: Clues to petrogenesis, dyke–flow relationships, and regional lava stratigraphy; *Bull. Volcanol.* **75** 701, https://doi.org/10.1007/s00445-013-0701-x.

Simpson F and Bahr K 2005 *Practical Magnetotellurics*; Cambridge University Press, Cambridge, https://doi.org/10.1017/CBO9780511614095.

Smith J T 1995 Understanding telluric distortion matrices; *Geophys. J. Int.* **122** 219–226.

Stagpoole V M, Bennie S L, Bibby H M, Dravitzki S and Ingham M R 2009 Deep structure of a major subduction back thrust: Magnetotelluric investigations of the Taranaki Fault, New Zealand; *Tectonophysics* **463** 77–85.

Swift C M 1967 A magnetotelluric investigation of an electrical conductivity anomaly in the southwestern United States; PhD Thesis, Massachusetts Institute of Technology, Dept. of Geology and Geophysics, http://hdl.handle.net/1721.1/38346.

Vijaya Kumar K, Chavan C, Sawant S, Raju K N, Kanakdande P, Patode S and Balaram V 2010 Geochemical investigation of a semi-continuous extrusive basaltic section from the Deccan Volcanic Province, India: Implications for the mantle and magma chamber processes; *Contrib. Mineral. Petrol.* **159** 839–862.

Vijaya Kumar K, Laxman M B and Nagaraju K 2017 Mantle source heterogeneity in continental mafic Large Igneous Provinces: Insights from the Panjal, Rajmahal and Deccan basalts, India; In: Large Igneous Provinces from Gondwana and Adjacent Regions (eds) Sensarma S and Storey B C, *Geol. Soc. London, Spec. Issue* **463** 87–116.

Vijaya Kumar P V, Patro P K, Rao P B V S, Singh A K, Kumar A and Nagarjuna D 2018 Electrical resistivity cross-section across northern part of Saurashtra region: An insight to crystallized magma and fluids; *Tectonophysics* **744** 205–214.

Vijaya Kumar P V 2020 Electromagnetic induction studies in Saurashtra region; PhD thesis, Andhra University, 158p.

Vozoff K 1991 The magnetotelluric method; In: *Electromagnetic Methods in Applied Geophysics,* Society of Exploration Geophysicists **2** 641–712, https://doi.org/10.1190/1.9781560802686.ch8.

Wannamaker P E, Doerner W M, Stodt J A and Johnston J M 1997 Subdued state of tectonism of the Great Basin interior relative to its eastern margin based on deep resistivity structure; *Earth Planet. Sci. Lett.* **150** 41–53, https://doi.org/10.1016/s0012-821x(97)00076-9.

Weaver J T, Agarwal A K and Lilley F E M 2000 Characterization of the magnetotelluric tensor in terms of its invariants; *Geophys. J. Int.* **141** 321–336.

Weidelt P 1977 Numerical study of a conductive channelling effect; *Acta Geodaet. Geophys. Montanist. Acad. Sci. Hung.* **12** 195–205.

Corresponding editor: Saibal Gupta